Axin expression in thymic stromal cells contributes to an age-related increase in thymic adiposity and is associated with reduced thymopoiesis independently of ghrelin signaling

Hyunwon Yang,* Yun-Hee Youm,* Yuxiang Sun,† Jong-Seop Rim,‡ Craig J. Galbán,§ Bolormaa Vandanmagsar,* and Vishwa Deep Dixit*,[1]

*Laboratory of Neuroendocrine-Immunology, ‡Division of Experimental Obesity, Pennington Biomedical Research Center, Louisiana State University System, Baton Rouge, Louisiana, USA; †Huffington Center on Aging, Baylor College of Medicine, Houston, Texas, USA; and §Radiology Department, University of Michigan, Ann Arbor, Michigan, USA

Abstract: The adipocytes are the predominant cell types that constitute the bulk of the thymic microenvironment by the fifth decade of life in healthy humans. An age-related increase in thymic adiposity is associated with reduced thymopoiesis and compromised immune surveillance in the elderly. However, the mechanisms regulating the generation of intrathymic adipocytes during aging remain to be elucidated. Here, we report that the CD45$^-$ thymic stromal cells (TSCs) are amenable to adipogenesis. We identified that the Wnt inhibitor axin is expressed in the lymphoid as well as stromal cells of the thymus with increased expression in CD45$^-$ TSCs of older mice. Knockdown of axin by RNA interference in CD45$^-$ primary TSCs led to a marked reduction in adipogenesis with significantly lower expression of adipogenic transcripts peroxisome proliferator-activated receptor γ2 (PPAR), adipocyte fatty acid-binding protein (aP2), and perilipin. Age-related elevated axin expression was increased specifically in thymic fibroblasts and medullary thymic epithelial cells (TECs) but not in the cortical TEC or CD45$^+$ cells. Consistent with a role of axin in promoting thymic adipogenesis, axin expression was also colocalized with lipid-expressing adipogenic cells in aging thymus. The prolongevity intervention, caloric restriction (CR), prevented the age-related increase in axin and the adipogenic cell in the thymus together with increase in thymic output. We have recently demonstrated that CR induces ghrelin, which can partially reverse thymic involution. Here, we show that axin expression is not affected by ablation of ghrelin receptors in aging mice, suggesting a ghrelin-independent mechanism for regulation of axin. Our data are consistent with the hypothesis that blocking the specific proadipogenic signals in the thymus may complement the present approaches to rejuvenate thymic function during aging. *J. Leukoc. Biol.* 85: 928–938; 2009.

Key Words: *aging · Wnt · adipogenesis · GH · adipocyte · dietary restriction · obesity*

INTRODUCTION

Deterioration of immune function with progressive aging is linked in large part to the reduced ability of thymus to produce naïve T cells [1]. The thymic involution process can be detected post-puberty and is associated with changes in the production of sex-steroid hormones [2]. It is presently unclear why thymic involution is initiated early on in life, but this maladaptive response has severe consequence for the immune responsiveness with progressive age [3]. Apart from circulating neuroendocrine factors regulating thymic function [4], the alteration in the thymic microenvironment [5–7], changes in intrathymic growth factors [8, 9], loss of lymphoid progenitors [10], and epithelial cell populations [11] are considered to play important roles in reduced thymic output with age.

The unique three-dimensional thymic meshwork is comprised of the cortex and medulla, composed mainly of distinct developing T cell subsets and thymic stromal cells (TSCs), which are a diverse group of cells including cortical thymic epithelial cells (cTECs), medullary TECs (mTECs), mesenchymal cells, fibroblasts, pericytes, endothelial cells, and adipocytes [12]. One of the hallmark changes in the thymic microenvironment with aging is a progressive increase in adipocytes in the thymic parenchyma, septa, cortex, and medulla with replacement of epithelial and T-lymphopoietic thymic zones into adipose tissue [3, 13–15]. The mechanisms responsible for the origin of adipocytes in thymus and their progressive deposition, such that they replace virtually all of the thymopoietic microenvironment with age, remain to be elucidated.

The Wnt pathway has been implicated in lineage-commitment and cell-fate regulation during development and aging [16, 17]. Axin is an integral component of the Wnt pathway and a product of the mouse-fused locus, which is known to be a negative regulator of Wnt signaling [18]. Axin is ubiquitously expressed during embryogenesis, and consistent with a integral

[1] Correspondence: Laboratory of Neuroendocrine-Immunology, Pennington Biomedical Research Center, Louisiana State University System, 6400 Perkins Rd., Baton Rouge, LA 70808, USA. E-mail: Vishwa.dixit@pbrc.edu

Received October 14, 2008; revised January 10, 2009; accepted February 2, 2009.

doi: 10.1189/jlb.1008621

role of axin in Wnt signaling machinery, the embryos lacking axin die at Embryonic Day 9.5 as a result of severe abnormalities in neural tube formation, forebrain development, and axis duplication [19]. Wnts are a family of paracrine and autocrine factors known to play a critical role in cell growth and differentiation, tissue morphogenesis, and cancer [20]. It appears that a central function of axin is to promote the phosphorylation of β-catenin by *glycogen synthase kinase 3* (GSK-3) [21]. According to the prevailing view of canonical Wnt signaling, in the absence of Wnt signals, GSK-3 phosphorylates axin, leading to the ubiquitination and degradation of cytosolic β-catenin [22]. In the presence of Wnt signals, GSK-3 activity is inhibited, causing hypophosphorylation of axin and preventing β-catenin from the degradation, allowing its accumulation and translocation to the nucleus to initiate transcription of target genes [21]. In contrast, noncanonical Wnt signaling functions in a β-catenin-independent manner via extracellular Wnt ligands and their interactions with frizzled receptors [23]. These interactions cause activation of specific G proteins and phospholipase C and turnover and release of intracellular calcium ions [22]. The canonical [24] and noncanonical Wnt pathway [25] has been shown to play an integral role in T cell development in the thymus [26, 27].

We have demonstrated recently that ghrelin, a stomach-derived anabolic peptide, can promote thymopoiesis during aging [4]. Interestingly, during the course of these studies, we observed that the ghrelin infusions reduced the neutral lipid-expressing adipocytes in the aging thymus, and ghrelin receptor (GHSR) knockout (KO) mice developed excess thymic adipocytes and exhibited reduced thymic output [4]. Here, we investigated the mechanism responsible for thymic involution with focus on specific adipogenic regulators that may provide inductive signals required for adipocyte development in the thymus. The focus of many of the current studies about Wnt proteins in thymocyte development and hematopoietic stem cells has led to identification of the critical function of these proteins in the thymus [28]. Considering a vital role played by Wnt inhibitors in aging and cellular differentiation, we hypothesized that the axin may regulate adipocyte development within the thymus and contribute to age-related thymic involution. Using in vitro and in vivo approaches, we provide evidence that the axin regulates adipogenic programming of the TSC, and an age-related increase in the thymic axin and reduced T cell output can be prevented by prolongevity intervention, caloric restriction (CR). Our data suggest that increased expression of the axin in the aging thymus may be one of the molecular triggers involved in regulating the process of age-related thymic adiposity.

MATERIALS AND METHODS

Thymic magnetic resonance imaging (MRI)

MRI examinations were performed on healthy subjects between 40 and 45 years of age ($n=12$) using Institutional Review Board-approved protocols with informed consent. The imaging was performed with subjects' head first, supine in a 3T full-body scanner (Signa, General Electric Medical Systems, Milwaukee, WI, USA). A body-surface receive-only coil and a full-body transmit coil were used to scan at the level of tracheal bifurcation. T_1-weighted spin echo axial images were performed using the following parameters: repetition time/echo time (TR/TE), 500/10 ms; slice thickness, 4 mm; field of view (FOV), 32 × 32 cm; matrix, 320 × 320 (resolution, 1×1 mm); 10 slices; and slice gap, 1 mm. T_2-weighted fast-spin echo axial images were done using the following parameters: TR/TE, 3000/80 ms; echo train, 8; slice thickness, 4 mm; FOV, 32 × 32 cm; matrix, 320 × 320; 10 slices; and slice gap, 1 mm. Total acquisition times for the T_1-weighted and T_2-weighted images were ~5 min and ~2 min, respectively; total examination time was ~7 min. To minimize image artifacts and increase thymus contrast, modification of both sequences may be necessary at the time of examination.

Mice

The female CR ($n=20$) mice and ad libitum (AL)-fed ($n=20$) 3-, 10-, 12-, and 18-month-old C57/B6 mice were purchased from a National Institute on Aging aging rodent colony (Harlan Sprague-Dawley, Indianapolis, IN, USA). CR was initiated at 14 weeks of age at 10% restriction, increased to 25% restriction at 15 weeks, and to 40% restriction at 16 weeks, where it is maintained throughout the life of the animal. Mice were maintained on the CR diet during transit and sacrificed after 1 day's rest. We also used 3- to 4-month-old female C57BL/6 mice as controls. The mice were maintained under pathogen-free conditions in the animal facility at the Pennington Biomedical Research Center (PBRC; Baton Rouge, LA, USA) using protocols approved by the PBRC Animal Care and Use Committee. The GHSR mice have been described previously [4]. The GHSR null mice have been backcrossed to C57B6 background for at least eight generations. A total of six to eight age-matched female wild-type (WT) and GHSR null mice was used for these experiments.

TSC culture and transfections

Thymic lobes were minced into small fragments and treated for 1 h at 37°C with an enzymatic mixture containing 1 mg/ml collagenase (Sigma Chemical Co., St. Louis, MO, USA), 0.2 mg/ml DNAse type I (Sigma Chemical Co.), and 1 mg/ml trypsin EDTA (Gibco, Grand Island, NY, USA) in PBS. The CD45 cells were depleted using magnetic bead-based positive selection as described previously [2, 11]. The CD45-negative fractions were resuspended, and 1×10^6 cells/well were seeded in six-well or 24-well culture plates and cultured for 14 days in DMEM nutrient F12 (DMEM/F12; with 15 mM HEPES, $NaHCO_3$, L-glutamine, Gibco), supplemented with 3 μg/ml insulin, 20 ng/ml epidermal growth factor (EGF), 100 U/ml penicillin-streptomycin, and 20% FBS. Cultures were maintained at 37°C and 5% CO_2. After cells reached 70% confluence, the TSCs were transfected by control and axin-specific small interfering (si)RNA using a lipofectamine-based kit based on the manufacturer's recommendation (Dharmacon, Chicago, IL, USA). Adipogenesis was induced by changing the medium to DMEM/F12 containing 10% FBS, 0.5 mM 3-isobutylmethylxanthine, 1 μM dexamethasone, and 1.7 μM insulin [multiple daily injections (MDI)].

Flow cytometry

The thymic fragments were digested enzymatically, and cells were labeled with CD45, anti-MHCII, Ly51, platelet-derived growth factor receptor α (PDGF-Rα; eBioscience, San Diego, CA, USA), MTS15, and isotype control IgG with appropriate secondary-conjugated antibodies. For intracellular axin staining, cells were fixed by paraformaldehyde and permeabilized using saponin. After blocking for nonspecific-binding sites, the cells were stained using secondary Alexa Fluor 488 (Invitrogen, Carlsbad, CA, USA) and allophycocyanin (APC)-conjugated anti-CD45 antibody. FACS sorting of TSC was performed on FACSAria as described previously [2]. The FACS analysis was performed on FACSCalibur, and data were analyzed by post-collection compensation using FlowJo (Tree Star Inc., Ashland, OR, USA) software.

Immunofluorescence staining

The whole thymi obtained from mice were stored in 2% sucrose in PBS overnight at 4°C. The tissues were embedded in OCT compound and frozen on a cryo-microtome specimen holder. Thick frozen sections (0.5–0.7 μm) were cut in a cryo-microtome, and at least three serial sections were used for each staining. Tissue sections were then fixed with cold ethanol and 4% buffered paraformaldehyde, and then nonspecific binding sites were blocked with protein-blocking buffer. After overnight incubations with unconjugated rabbit polyclonal anti-human axin (H-98, Santa Cruz Biotechnology, Santa Cruz, CA,

USA), unconjugated rat antibody to ERTR7 (HM1086, Cell Sciences, Canton, MA, USA), or unconjugated rabbit antibody to fibroblast-specific protein-1 (FSP-1; ab27957, Abcam, Cambridge, MA, USA), the sections were labeled with Alexa Fluor 594-conjugated polyclonal chicken anti-rabbit IgG secondary antibody or Alexa Fluor 488-conjugated polyclonal donkey anti-rat IgG (Invitrogen). In addition, for the visualization of lipid droplet and adipocyte populations, frozen thymic sections and cultured cells were fixed with 4% buffered paraformaldehyde and then stained with LipidTOX Green (Invitrogen) for 20 min. Negative controls, as obtained by occulting the primary antibody or by using an unrelated IgG, displayed no specific labeling. Fluorescence mounting solution (Vector, Burlingame, CA, USA) was applied to slides and observed with a Zeiss Axioplan 2 microsocpe.

Western blot analysis

Thymi were lysed in radioimmune precipitation assay buffer supplemented with a protease and phosphatase inhibitor mixture (Sigma Chemical Co.), and protein concentrations of cell lysates were determined. The lysates were diluted with sample buffer, separated on 4–20% Tris-HCl/SDS-polyacrylamide gels (Novex, Wadsworth, OH, USA), and electrophoretically transferred to nitrocellulose membranes (Invitrogen). The blots were then incubated with rabbit polyclonal anti-human axin (H-98, Santa Cruz Biotechnology) antibody, rabbit polyclonal anti-mouse β-catenin or goat polyclonal anti-mouse Wnt-10b (N-19, Santa Cruz Biotechnology), and actin-specific mouse mAb (Sigma Chemical Co.). Immune complexes were visualized by incubation with specific secondary antibodies conjugated to Alexa Fluor 680 or IRDye® 800CW-conjugated affinity-purified anti-mouse IgG (Rockland Immnunochemicals, Gilbertsville, PA, USA), and then membranes were imaged for fluorescence on an Odyssey infrared imaging system (LI-COR Biosciences, Lincoln, NE, USA). The quantification of Western blots was performed using ImageJ software from the National Institutes of Health (NIH; http://rsb.info.nih.gov/ij/index.html).

Real-time RT-PCR

Total RNA was prepared with RNAzol (Iso-Tex Diagnostics, Friendswood, TX, USA). The cDNA synthesis and real-time RT-PCR were performed as described previously [4]. Real-time RT-PCR analyses were done in duplicate on the ABI PRISM 7900 sequence detector *Taq*Man system with the SYBR Green PCR kit as instructed by the manufacturer (Applied Biosystems, Foster City, CA, USA). The following primer pairs were used: GAPDH forward (5′-TTGATGGCAACAATCTCCAC-3′) and reverse (5′-CGTCCCGTAGACAAAATGGT-3′), axin forward (5′-CCCCCATACAGGATCCGTAA-3′) and reverse (5′-GGTACCCGCCCATTGACTT-3′), peroxisome proliferator-activated receptor γ (PPARγ) forward (5′-ACAAGACTACCCTTTACTGAAATTACCAT-3′) and reverse (5′-TGCGAGTGGTCTTCCATCAC-3′), PPARγ2 forward (5′-GCCTATGAGCACTTCACAAGAAATT-3′) and reverse (5′-TGCGAGTGGTCTTCCATCAC-3′), adipocyte fatty acid-binding protein (aP2) forward (5′-GCGTGGAATTCGATGAAATCA-3′) and reverse (5′-CCCGCCATCTAGGGTTATGA-3′), perilipin forward (5′-GACACCACCTGCATGGCT-3′) and reverse (5′-TGAAGCAGGGCCACTCTC-3′), Naked 1 (Nkd1) forward (5′-GGGAAACTTCACTCGAAGCC-3′) and reverse (5′-ACTCCTCGATGCCTTTCCTT-3′), preadipocyte factor 1 (Pref-1) forward (5′-TTCGGCCACAGCACCTATG-3′) and reverse (5′-ACATTGTCAGCCTCGCAGAA-3′), C/EBP homologous protein (CHOP) forward (5′-CAGCGACAGAGCCAGAATAA-3′) and reverse (5′-GACCAGGTTCTGCTTTCAGG-3′), Kruppel-like factor 6 (KLF6) forward (5′-CACGAAACGGGCTACTTCTC-3′) and reverse (5′-ACACGTAGCAGGGCTCACTC-3′), and IL-7 forward (5′-GGGAGTGATTATGGGTGGTGAG-3′) and reverse (5′-TGCGGGAGGTGGGTGTAG-3′).

Quantification of signal joint TCR excision circles (sjTRECs)

CD4+ T subsets were isolated from splenocytes using the mouse CD4+ T cell positive section kit (Invitrogen). The sorted cells were lysed in 100 mg/L proteinase K (Sigma Chemical Co.) for 1 h at 56°C followed by 10 min at 95°C. The amount of TRECs in 5×10^6 cells was determined by real-time quantitative PCR using the ABI PRISM 7900 sequence detector *Taq*Man system (Applied Biosystems). The PCR performed with mδRec- and ψJα-specific primers and mδRec-ψJα fluorescent probe as described previously [4]. The standard curves for murine were generated by using δRec and ψJα TREC PCR product cloned into a pCR-XL-TOPO plasmid, a generous gift from Dr. Gregory Sempowski, Duke University Medical Center, Durham, NC, USA.

Statistical analysis

The values given in this article are presented as mean ± SEM. All analyses were performed by ANOVA followed by a Fisher's least significant difference test using Sigma Stat software. $P < 0.05$ was viewed as statistically significant.

RESULTS

Thymic adiposity in healthy humans

The histological analysis of human thymus shows a marked increase in adipocytes with increasing age within the thymic microenvironment, suggesting a potentially prominent role played by fat cells in the age-related thymic involution process [13, 14]. Given that the lymphoid and adipose tissue can be distinguished from each other as a result of differences in water content and proton relaxation, we sought to investigate the phenomenon of adipocyte accumulation in 40- to 45-year-old healthy human ($n=12$) thymi using MRI. Two image modalities were used for thymus volume measurements in this study: T_1-weighting and T_2-weighting. These modalities provide ample tissue contrast and require short acquisition times. Given that the T_1 relaxation times for water is much longer than that of fat, MRI can analyze the presence of lipid within the thymus.

As evident from the images in **Figure 1A**, our thymic MRI protocol is sensitive to detect the changes in the thymic volumes and fat infiltration. The region of interest (ROI) depicting the thymus is highlighted in red. The images were acquired at the level of tracheal bifurcation and show trapezoidal-shaped thymus located anterior to the sternum and posterior to the ascending aorta. The T_1 of fat is much shorter than water, resulting in less saturation and more signal from fat in a T_1-weighted sequence (Fig. 1B). A hyperintense region within the thymus is attributable to fat accumulation, and thymic remnants are visible as a pale area within the ROI, which was selected based on the criteria published previously [29]. Analysis of cryosections of 18-month-old murine thymi demonstrated the presence of lipid-expressing cells; interestingly, we noted that the Wnt regulator axin was colocalized with adipogenic cells in the aging thymus (Fig. 1C).

Axin regulates adipogenesis of TSCs

Axin is believed to be a ubiquitously expressed gene [18, 19]. However, expression of axin in specific thymic cell populations and regulation with aging remain to be determined. Based on our initial observation that axin is colocalized in adipogenic stromal-like cells in the thymus, we next quantitated the axin expression in thymic cells using FACS and immunohistochemical analyses. The FACS analysis of thymus revealed that in young animals, axin protein is expressed at a higher frequency in $CD45^+$ cells. Interestingly, an age-related increase in axin expression was detected in the $CD45^-$ stromal cells (**Fig. 2, A** and **B**). Given the sensitivity and limits associated with detection of intracellular proteins, such as axin, using FACS analysis, we next quantitated the axin gene expression in $CD45^-$-sorted TSC populations. The thymi from young ($n=6$) and 12-month-old ($n=6$) mice were digested enzymatically, and thymocytes were depleted using anti-CD45 magnetic bead-based methods. The pooled $CD45^-$ cell fraction was used

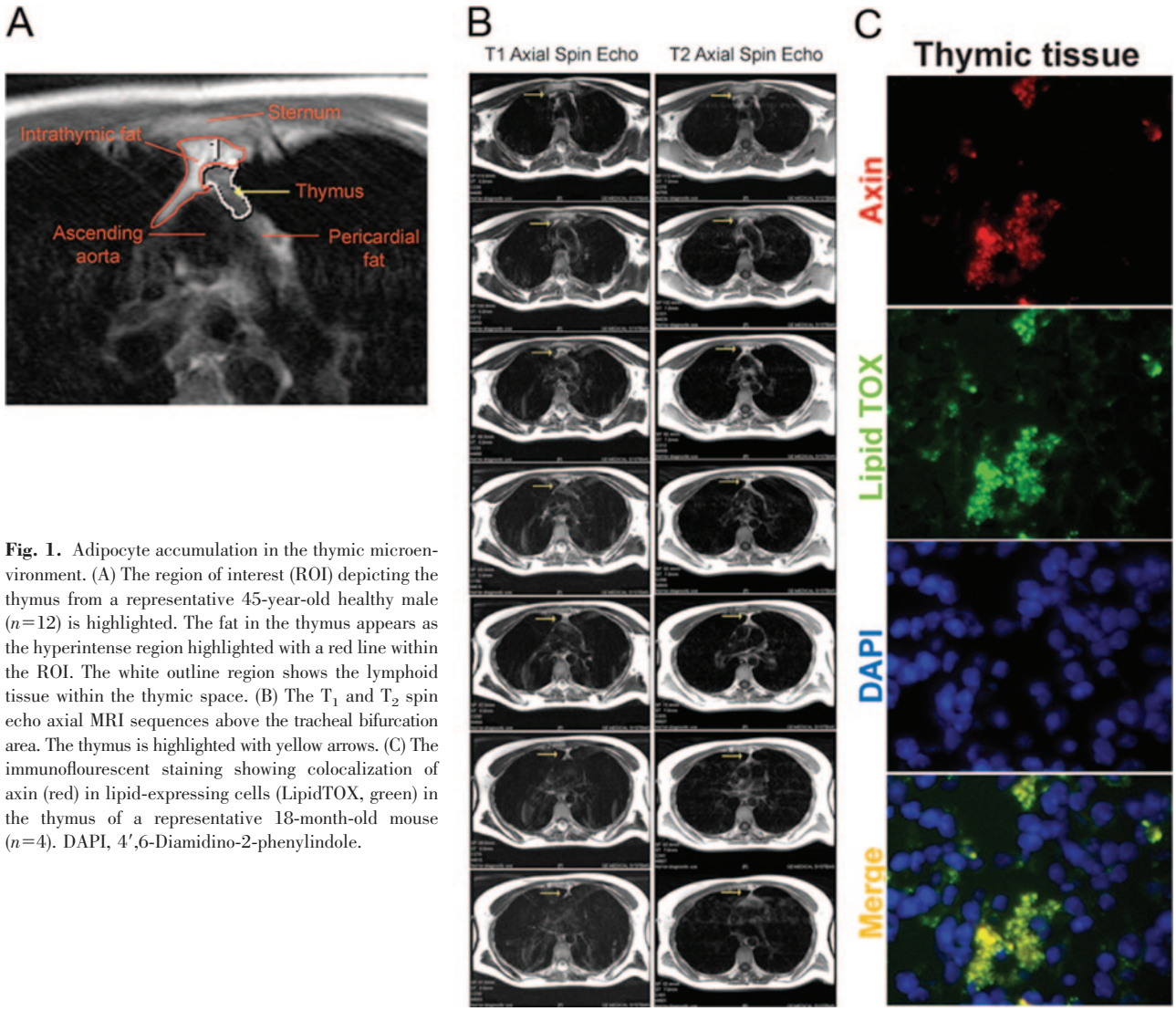

Fig. 1. Adipocyte accumulation in the thymic microenvironment. (A) The region of interest (ROI) depicting the thymus from a representative 45-year-old healthy male (n=12) is highlighted. The fat in the thymus appears as the hyperintense region highlighted with a red line within the ROI. The white outline region shows the lymphoid tissue within the thymic space. (B) The T_1 and T_2 spin echo axial MRI sequences above the tracheal bifurcation area. The thymus is highlighted with yellow arrows. (C) The immunoflourescent staining showing colocalization of axin (red) in lipid-expressing cells (LipidTOX, green) in the thymus of a representative 18-month-old mouse (n=4). DAPI, 4′,6-Diamidino-2-phenylindole.

subsequently to sort the mTEC ($CD45^-MHCII^+Ly51^-$), cTEC ($CD45^-MHCII^+Ly51^+$), and thymic fibroblasts (TF; $CD45^-PDGF\text{-}R\alpha^+MTS15^+$). The real-time PCR analysis in sorted TSC populations revealed no changes in axin expression in cTECs. Interestingly, an age-related increase in axin expression in mTEC and TF cells was detected (Fig. 2C).

We next tested the hypothesis that axin expression regulates the adipogenesis of primary TSCs. The $CD45^-$ TSCs from 2-month-old mice were isolated and grown in culture and allowed to reach 70% confluence. The TSCs were transfected with scrambled control and axin-specific siRNA, and 48 h post-transfection, these cells were exposed to an adipogenic cocktail containing methylisobutylxanthine (0.5 mM), dexamethasone (1 μM), and insulin (1.67 μM) and cultured for an additional 48 h. We demonstrate that compared with control-transfected cells, the axin siRNA down-regulated the axin mRNA expression efficiently (**Fig. 3A**). We observed that upon MDI treatment, the control siRNA-transfected cells differentiated into adipocytes, as assessed by rounding and development of lipid vacuoles (Fig. 3B). Interestingly, the axin-deficient TSCs were resistant to MDI-induced adipogenic transformation (Fig. 3B).

The adipocyte differentiation requires regulated expression of specific proadipogenic genes and transcription factors [30, 31]. It is well known that γ1 and γ2 isoforms of PPAR, generated as a result of alternative splicing and promoter use, are induced upon adipogenesis and are required for the maintenance of the differentiated state of the adipocyte [32, 33]. In addition, aP2 and perilipin are required for adipogenesis [31, 34]. We found that axin-deficient TSCs displayed reduced adipogenesis and expressed significantly lower levels of PPARγ, PPARγ2, aP2, as well as perilipin (Fig. 3C). These findings demonstrate that axin regulates the adipogenesis of TSC in vitro and age-related increase in axin expression in TSC, and fibroblast may contribute to thymic adipogenesis.

Age-related increase in axin expression in TF and lipid-bearing cells is blocked by CR

The histological hallmark of thymic involution is loss of thymocyte and adipocyte accumulation in the thymic space that eventually replaces the lymphoid and stromal cell compartment with adipose tissue [13, 14]. Axin has been demonstrated previously to play an important role in promoting adipogenesis

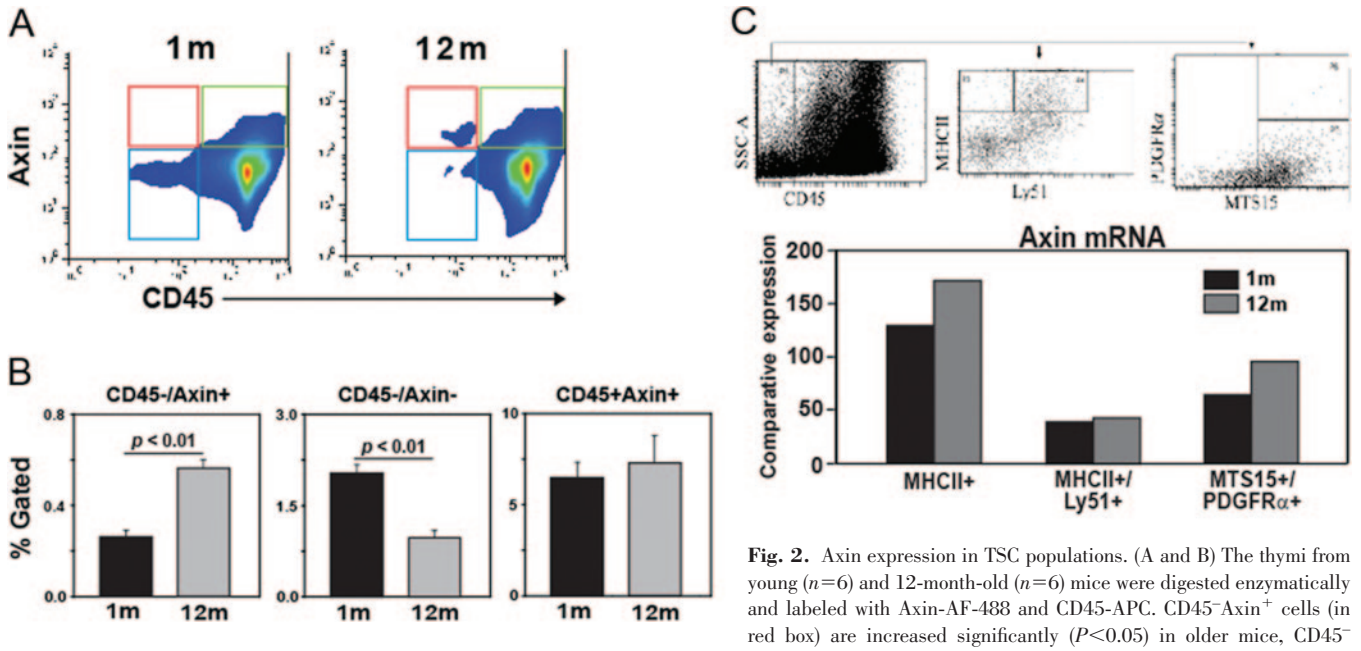

Fig. 2. Axin expression in TSC populations. (A and B) The thymi from young ($n=6$) and 12-month-old ($n=6$) mice were digested enzymatically and labeled with Axin-AF-488 and CD45-APC. $CD45^{-}Axin^{+}$ cells (in red box) are increased significantly ($P<0.05$) in older mice, $CD45^{-}Axin^{-}$ (blue box) decrease with age, and no change in $CD45^{+}Axin^{+}$ (green box) is detected. All data are expressed as mean ± SEM. (C) The CD45 cells were depleted from thymic digests using magnetic bead-based positive selection. The $CD45^{-}$ cells from six thymi, each from 2- and 12-month-old mice were pooled and used for sorting the mTEC ($CD45^{-}MHCII^{+}Ly51^{-}$), cTEC ($CD45^{-}MHC11^{+}Ly61^{+}$), and fibroblasts ($MTS15^{+}PDGF\text{-}R\alpha^{+}$). The comparative threshold values from triplicate real-time PCR analyses were collapsed together, and data are expressed as relative axin mRNA expression. SSC-A, Side-scatter-A.

of the cultured 3T3-L1 fibroblast cell line [34]. Given that Wnt signaling has a prominent role in aging and regulates cell-fate determination [35–37] and our initial findings that axin is colocalized in adipogenic cells in thymus and expressed in $MTS15^{+}PDGF\text{-}R\alpha^{+}$ TF prompted us to study the axin localization further within the aging thymic microenvironment. Furthermore, we hypothesized that prolongevity intervention, CR, a state of chronic negative energy balance, will prevent axin-induced adipogenic changes in aging thymus. Compared to young mice (3 months), the thymi of 18-month-old animals showed a large increase in axin-expressing and lipid-bearing cells (**Fig. 4**). Furthermore, axin was found to be co-expressed in greater frequency with neutral lipid-containing cells in thymus. Interestingly, the thymi from CR animals displayed axin and lipid expression patterns similar to a 3-month-old mouse (Fig. 4), suggesting that lower thymic axin expression is associated with reduced ectopic adipocyte accumulation in thymic space.

Given that fibroblasts are highly plastic and can differentiate efficiently into adipocytes, we studied the axin expression in TF. Compared with young animals (3 months), we detected an increase in the $ERTR7^{+}$ fibroblast in 12-month-old mice (**Fig. 5A**), which was prevented by CR in age-matched animals. Consistent with our FACS data, we observed that axin expression was increased in older mice and was partially colocalized with $ERTR7^{+}$ fibroblasts (Fig. 5A). We also studied the localization of axin in a subset of fibroblast specific protein-1 (FSP-1)-expressing secondary mesenchymal cells. FSP-1 has been demonstrated to be expressed constitutively and selectively in the newly formed fibroblasts [38, 39]. Similar to ERTR7, we found that axin is also expressed in FSP-1-expressing TF (Fig. 5B). Together, these data suggest that physiological aging leads to increased axin expression within the adipogenic TSCs, including the TF populations.

Inhibition of axin expression by CR is associated with an increase in recent thymic emigrants (RTEs)

We next quantified the total thymic axin expression during aging and upon CR. Compared to young mice, the intrathymic axin mRNA as well as protein expression was significantly increased in 12- and 18-month-old mice (**Fig. 6, A** and **B**). Consistent with our data from immunofluorescent analysis of thymic cryosections, we found that CR robustly prevented the age-related increase in axin expression (Fig. 6, A and B). In an effort to understand the consequence of CR-induced inhibition of an age-related increase in axin on thymopoiesis, we next quantified the TRECs in the peripheral $CD4^{+}$ cells. The T cells expressing TRECs are considered as RTEs [40]. The T cells expressing the TCRαβ emigrate from the thymus, and as TRECs are stable and do not replicate, their presence in T cells is used to distinguish the RTEs from pre-existing, naïve T cells. It should, however, be noted that analysis of TRECs as an absolute measure of thymopoiesis is imperfect, as long-lived, naïve T cell populations can still carry TREC episomal DNA circles. In addition, half of the cells that have undergone a division after rearrangement can no longer be identified as RTEs [41]. However, mathematical models have demonstrated that decreased thymic output is reflected sufficiently in reduction of TREC levels [41]. Indeed, the TRECs decline by fivefold from birth to 35 years of age and up to 50-fold by age 65 [41], and in the absence of precise surface markers to identify RTEs, TREC measurement remains a surrogate marker of thymopoiesis. Consistent with these data, we observed that aging led to a significantly reduced number of

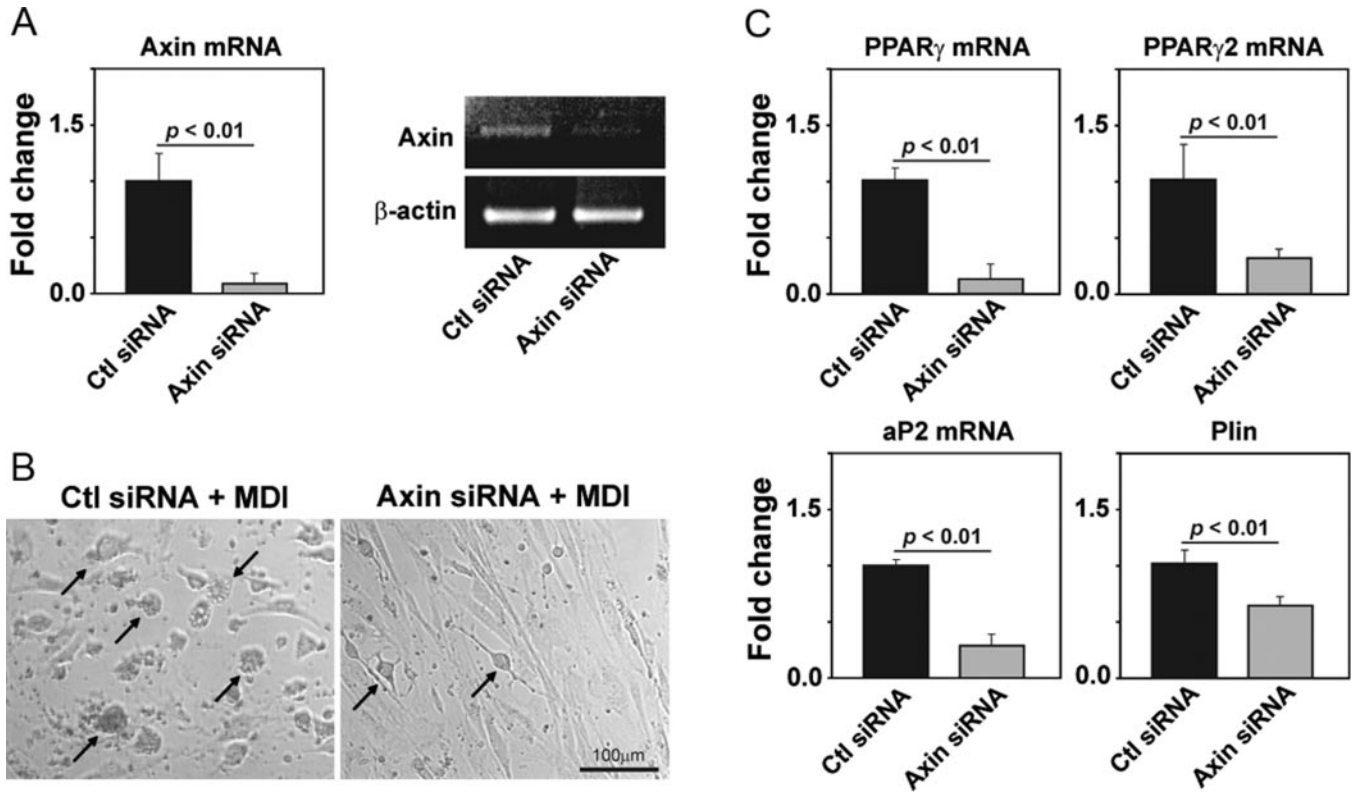

Fig. 3. Axin promotes adipogenesis of TSCs. (A) Real-time PCR analysis of axin in control (Ctl) and axin siRNA-transfected primary TSC cells. (B) Forty-eight hours post-siRNA transfections, the TSCs were treated with an adipogenic MDI cocktail. The control cells differentiated efficiently into adipocytes 28 h post-MDI exposure, and axin-deficient TSC displayed reduced adipogenic transformation. (C) The real-time PCR analysis of proadipogenic transcripts PPARγ, PPARγ2, aP2, and perilipin (Plin) in control and axin siRNA-transfected cells. The experiments were performed in duplicate wells and repeated thrice. All of the data are expressed as mean ± SEM.

TRECs (Fig. 6C). Interestingly, chronic CR in 10-month-old mice blocked the age-related decline in thymopoiesis and maintained the TREC counts to the levels observed in young 4-month AL-fed animals (Fig. 6C). Collectively, these data suggest that an inhibition of axin expression in the thymus is associated with increased thymic output.

As we observed strong effects of aging on axin expression in the thymus, we next investigated the components of Wnt signal machinery. The mRNA analysis of expression of Nkd1, a negative regulator of the canonical Wnt–β-catenin-T cell factor signaling pathway [42, 43], revealed no increase with aging, but CR inhibited the expression of Nkd1 in the thymus (**Fig. 7B**). Furthermore, aging and CR had no significant effect on the thymic β-catenin and Wnt10b total protein levels (Fig. 7A), suggesting potential involvement of the noncanonical Wnt pathway.

Given an increase in proadipogenic Wnt regulator axin in aging, we also evaluated the specificity of adipogenic programming in the thymus by studying the other known adipogenic genes, Pref-1, CHOP, and KLF6 [31], in the thymus. We observed that thymic aging is not associated with any changes in CHOP, KLF6, or IL-7 expression (Fig. 7C). Interestingly, we detected a significant decrease in Pref-1 expression in the aging thymus. The preadipocyte factor-1 (Pref-1) gene belongs to the Notch/Delta/Serrate family of EGF-like repeat-containing proteins and is known to inhibit adipogenesis [44–46]. The observed reduction in Pref-1 along with elevated axin expression in aging thymus are consistent with our hypothesis that specific adipogenic programming results in thymic adiposity. Furthermore, CR exerts specific effects on adipogenic genes, such as axin, but appears not to affect the negative adipogenic Pref-1 regulatory network.

CR induced reduction in axin expression is not mediated by ghrelin signaling

It is well-recognized that rodents on a CR diet display enhanced food-seeking behavior in an effort to make up for the reduction in caloric intake [3]. Ghrelin is a potent stomach-derived acylated peptide that induces food intake [4]. We have recently demonstrated that in 10- to 12-month-old mice, the CR diet causes elevation in gastric ghrelin production, resulting in high circulating levels of this orexigenic peptide [47]. In addition, our previous studies demonstrate that ghrelin infusion in aging mice reduces lipid-positive cells in the thymus, and GHSR null mice have increased adipocyte deposition in the thymus and display accelerated age-related thymic involution [4]. Therefore, we next asked the question whether elevated axin expression in GHSR-deficient mice contributes to thymic involution and investigated if ghrelin-receptor (GHSR) mediated signaling is involved in regulating thymic axin expression during aging. The GHSR knockout and control wild type (WT) mice were aged for 10 months, and axin expression was studied in the thymus and primary TSCs of these mice. Compared with age-matched WT animals, we did

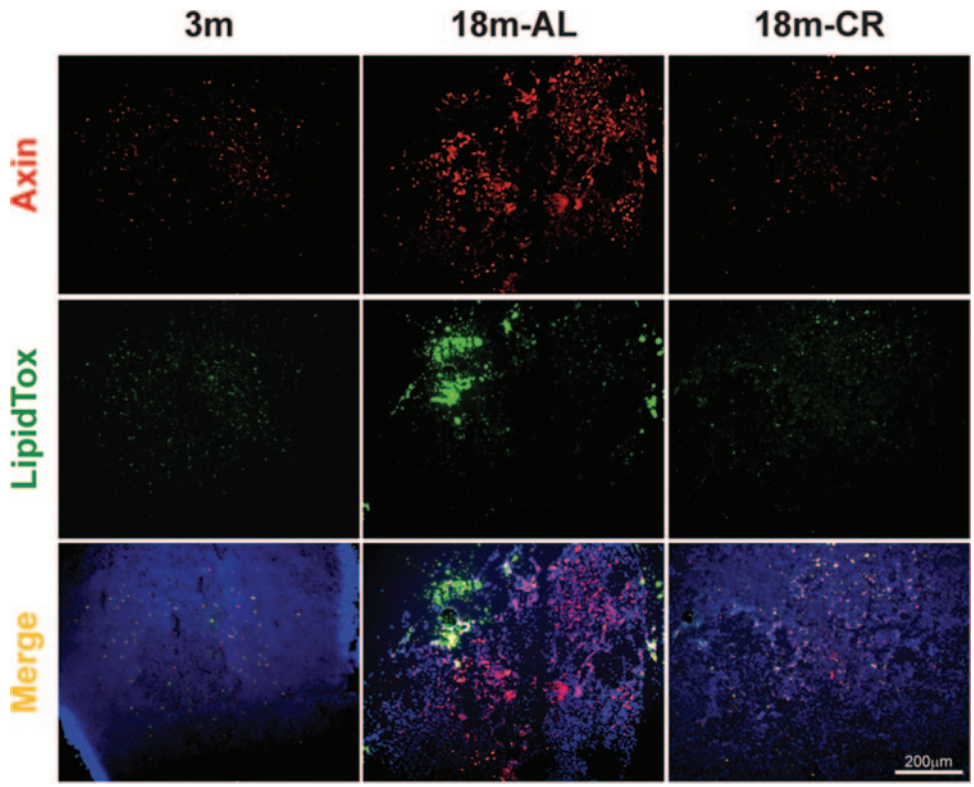

Fig. 4. Increased axin expression in the thymus is associated with thymic adiposity. The neutral lipid-expressing cells in thymic cryosections ($n=4$/age group) were stained for neutral lipid with LipidTOX (green) and anti-rabbit Axin antibody conjugated with Alexa Fluor 594 (red). The axin colocalizes with lipid-expressing cells in the thymus, as well as nonadipogenic thymic cells in aging mice.

not observe any change in axin-expressing cells or thymic axin mRNA expression in the 10-month-old GHSR–/– mice (**Fig. 8**). In addition, the TSCs from WT and GHSR–/– mice showed no difference in the axin mRNA expression (Fig. 8B). These data suggest that regulation of axin during aging is likely mediated via a ghrelin-independent mechanism, and thymic adipogenesis in ghrelin null animals may be mediated by distinct adipogenic pathways.

DISCUSSION

According to the prevailing view, the mechanisms responsible for reduced, naïve T cell production from aging thymus involve defects in lymphoid progenitors [10, 48], TECs [5, 49], thymocyte subsets, loss of intrathymic growth factors [9], and alteration in neuroendocrine [3, 4] and sex-steroid hormones [2]. Considering that the thymus undergoes almost complete "lipomatous atrophy" with age [13], we studied the changes in the thymic microenvironment and the role of the Wnt regulator axin in the aging thymus. We identified that axin regulates adipogenesis of TSCs and axin is markedly elevated in the aging thymus. These results led us to test whether the anti-aging intervention CR regulates Wnt signals and adipogenic progression in aging thymus. Our data suggest that CR inhibits adipocyte accumulation, increases thymic output, and inhibits axin expression in aging thymus.

In contrast to a young thymus, where thymocytes are the major contributors to the thymic environment, the situation is reversed in aging, where the adipocytes constitute the bulk of the microenvironment. Despite these dramatic changes, the aging thymus retains limited capacity for generating naïve T cells until late in life [50], suggesting that the improvement of thymic function is achievable. We have demonstrated recently that thymic regeneration in aged mice supplemented with exogenous ghrelin leads to reduction in lipid-expressing preadipocyte cells [4]. Furthermore, the GHSR KO mice express a greater number of adipocytes in the thymus and have reduced thymic output [4]. These data further suggest that the presence of thymic adipocytes is negatively related to the ability of thymus to produce naïve T cells. It is known that the reduction in thymocyte numbers precedes the development of adipocytes during aging. Whether the generation of thymic adipocytes with progressive aging is cause or consequence of thymic involution is still unclear. However, our findings provide clear evidence that primary thymic stromal elements can undergo adipogenic transformation, a process that can be attenuated by specific down-regulation of the axin. Given that TSCs are required for various aspects of T cell development, it is plausible that adipogenic transformation of these cells with age may lead to reduced thymopoiesis (**Fig. 9**).

Considering that the thymus lacks a pool of self-renewing progenitors, the early thymocyte progenitor (ETP) import via the high endothelial venules at the cortico-medullary junction is required for thymopoiesis [12, 51]. The subsequent generation of naïve T cells from ETPs in the thymus is critically dependent on the TSCs, in particular, mTEC and cTEC [49]. It has also been reported that age-related loss of thymic function is a result of reduction in and defects in the thymic epithelial compartment instead of defects in hematopoietic progenitors [5, 6]. Our data suggest that an age-related increase in axin expression on lipid-expressing fibroblasts may be an important determinant in compromising the thymic microenvironment required for thymopoiesis. Consistent with our findings during

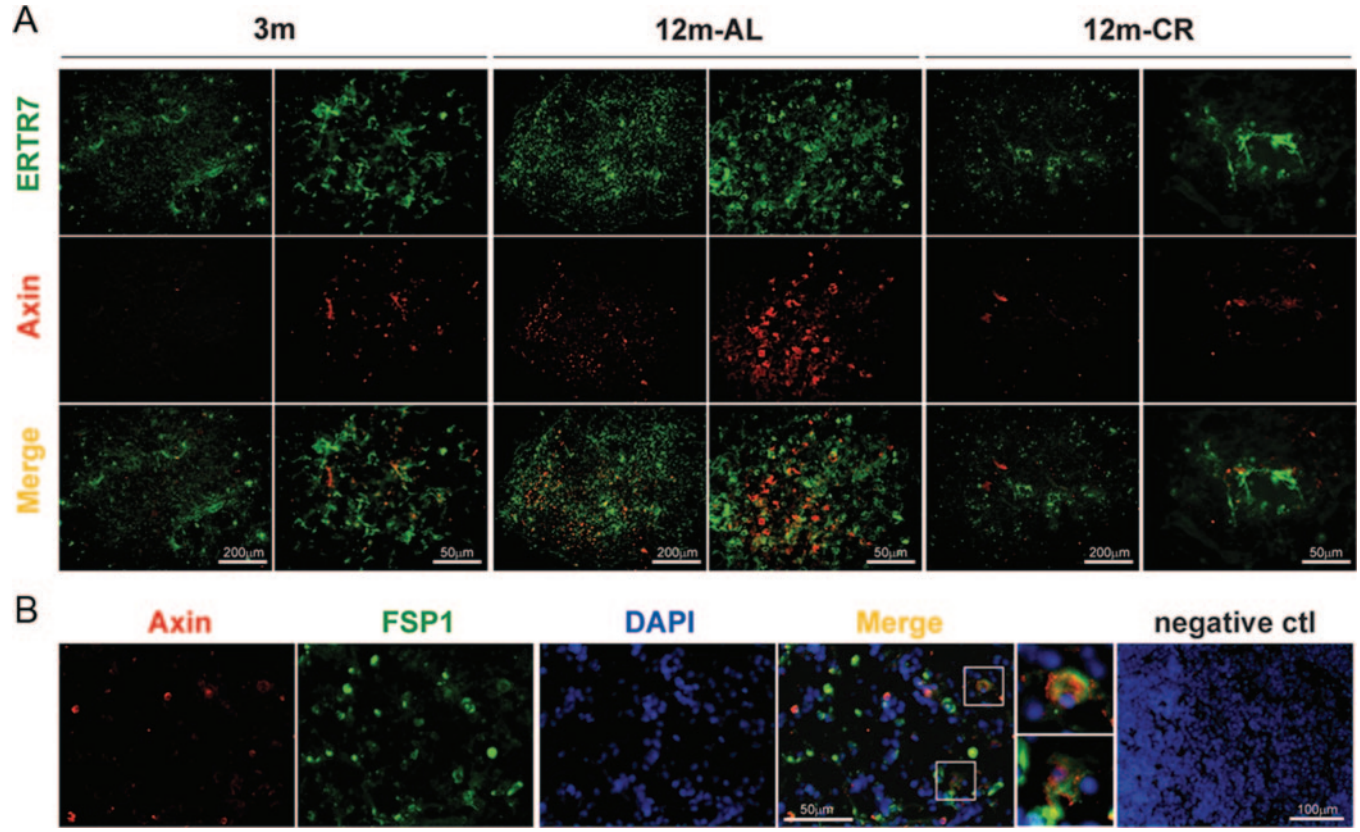

Fig. 5. Age-related increase in axin-expressing TF is blocked by CR. (A) TF were stained with ERTR7, followed by specific secondary antibody labeled with Alexa Fluor 488 (green), and axin was visualized by Alexa Fluor 594 (red)-conjugated antibody. The elevated axin expression in 12-month-old thymus colocalized with ERTR7. Representative images (original, 200×) of thymic sections of four mice in each group are shown. (B) Axin also partially colocalizes with FSP-1-expressing TF. The negative isotype IgG control antibody displayed no specific staining in the negative control cryosections of young and old mice.

aging, the axin-overexpressing transgenic mice have severe thymic involution [52]. Interestingly, the overexpression of the axin in mice also leads to increased mammary epithelial cell apoptosis and reduced pan-cytokeratin staining in the thymus [52], suggesting a potential role of the axin in TSC function. We quantitated and detected a specific increase in axin expression in TSCs. Furthermore, this high expression was restricted to mTEC and TF cells. Our data provide evidence that TSCs possess adipogenic potential and that axin may be one of the genes that promotes the adipocyte development in aging thymus. Together with previous findings that overexpression of axin in fibroblasts causes their differentiation into lipid-ex-

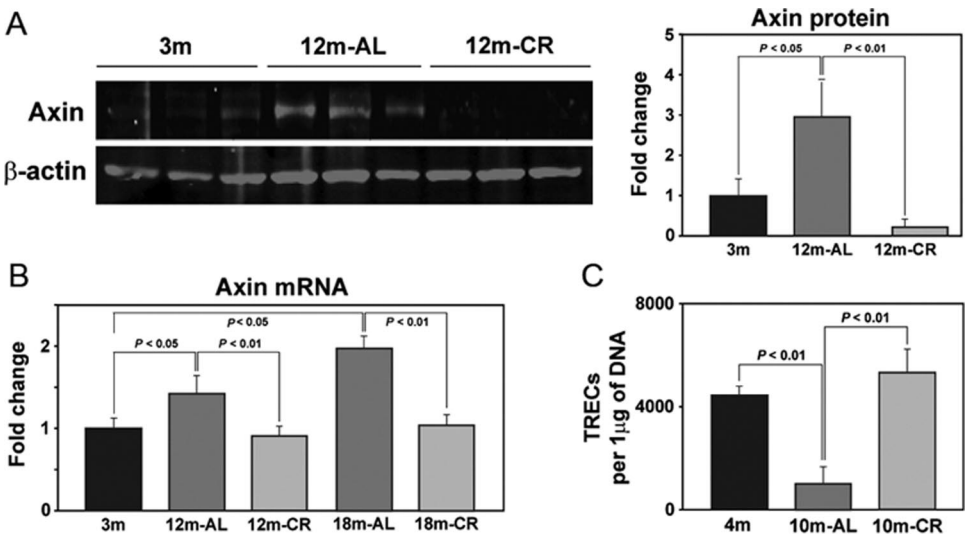

as mean ± SEM.

Fig. 6. Age-related increase in axin expression is prevented by chronic CR. (A) Quantitation of axin expression by Western blot of total thymic protein lysates displayed a marked increase in axin protein expression with age, and CR maintains the thymic axin to the levels observed in young animals. (B) The real-time PCR analysis of thymic axin mRNA in young and old mice. The age-matched CR mouse thymi revealed significantly ($P<0.05$) reduced axin expression in 12- and 18-month thymi ($n=6$/group). The data are expressed as mean ± SEM. (C) The splenic CD4 cells were isolated to prepare the DNA. Compared with AL-fed 4-month-old mice, the 10-month-old animals displayed a significant reduction in the sjTRECs, suggesting a reduced thymic cell output. The 10-month-old mice on a CR diet displayed a significant increase in the sjTRECs. A total of eight mice/group was used for TREC real-time PCR analysis. The data are expressed

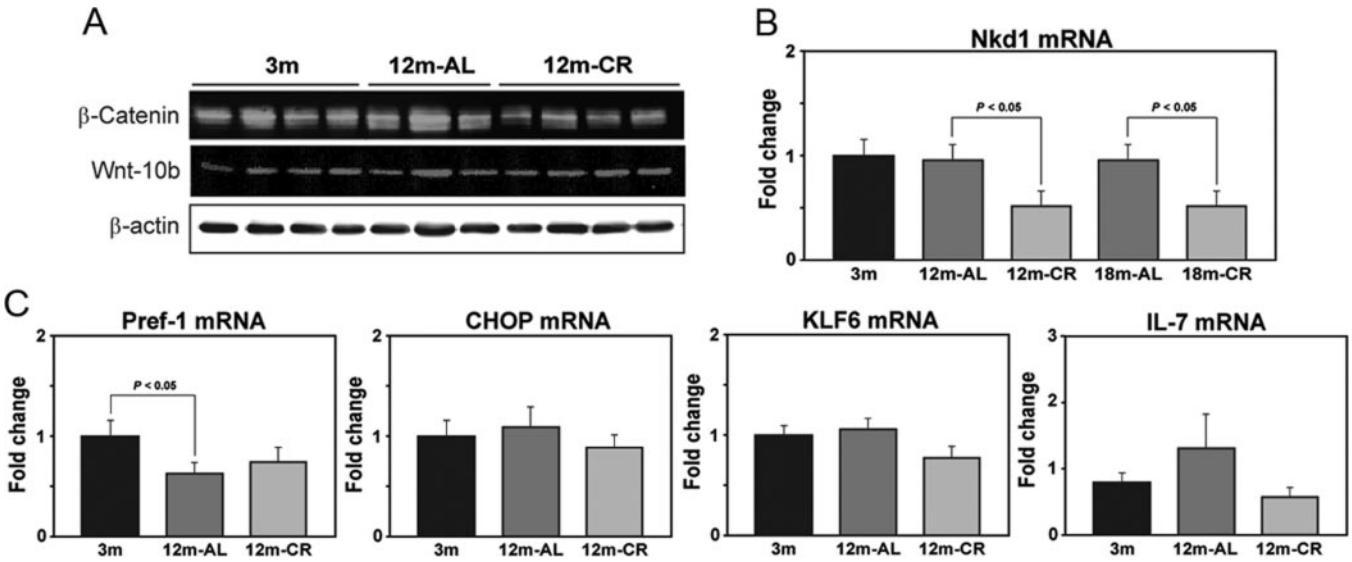

Fig. 7. Regulation of Wnt and adipogenic genes during aging and by CR. (A) Western blot analysis of β-catenin and Wnt10b in the thymus did not show any significant changes. (B) Thymic mRNA expression of Wnt antagonist Nkd1 in mice is not affected by age ($n=6$). (C) The real-time PCR analysis of adipogenic transcripts in the thymus shows that aging leads to a significant ($P<0.05$) reduction in Pref-1 without affecting CHOP and KLF6 mRNA expression. Compared with 3-month-old mice, no differences in IL-7 mRNA were observed in 12-month AL- and CR-fed mice.

pressing adipocytes [34], our present data suggest an important role for the axin in inducing adipogenesis of TF with increasing age. However, detailed lineage-tracing studies are required to address definitively the precise cellular origin and mechanisms of generation of thymic adipocytes during aging. Given that fibroblasts are unable to support T cell development of lymphoid progenitors [53], the increase in lipid-expressing fibroblasts may also be responsible for compromising the thymic microenvironment with age.

The CR-associated negative energy balance is the only preventive strategy that prolongs a healthy lifespan and attenuates age-related deficits in T cell output in primate models [54, 55]. The age-related increase in the Wnt inhibitor, axin, was blocked by CR and was associated with increased thymopoiesis. Given the broad systemic effects of CR, it is possible that extrinsic factors altered by CR, such as ghrelin, insulin-like growth factor 1, or sex steroids, may affect the thymic axin expression indirectly. As GHSR null mice do not have altered thymic axin expression, it is likely that CR-induced ghrelin release does not mediate axin expression. However, our findings suggest that reduction of axin expression in aging is associated with improved thymic output. The axin null mice are embryonically lethal, so a TSC-specific deletion of axin and subsequent aging of these genetic models may provide direct causal evidence for a role of this gene in thymic involution and thymoadipogenesis. Furthermore, considering that negative energy balance elicited by CR affects multiple pathways, the increased thymopoiesis in CR mice is not solely a result of down-regulation of axin expression. However, given our findings that axin knockdown in TSCs prevents their differ-

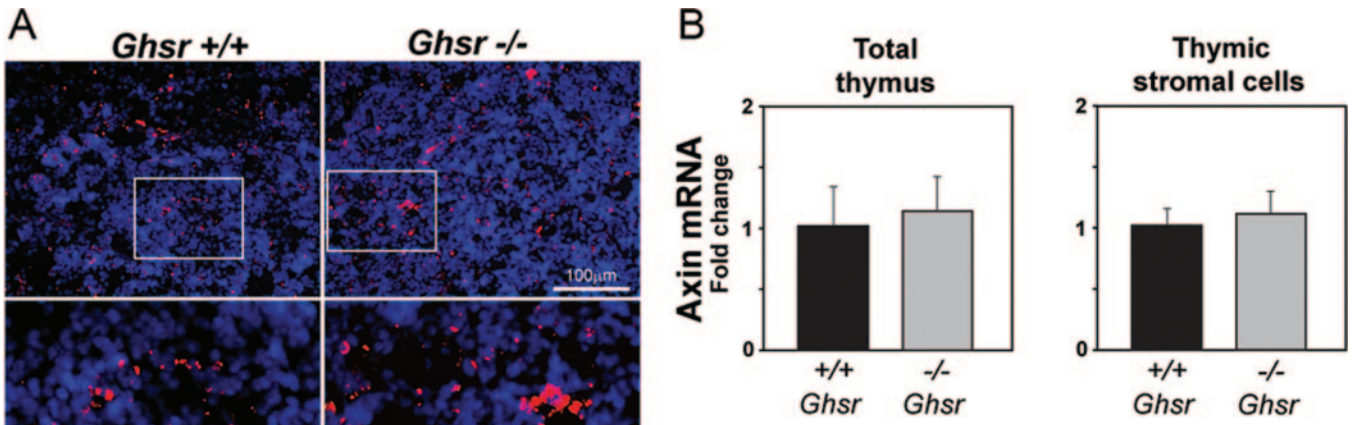

Fig. 8. Ghrelin signaling does not regulate age-related changes in thymic axin expression. (A) The 12-month-old GHSR KO and WT mice thymic cryosections were labeled with axin (10× original magnifications), and nuclei were counterstained with DAPI. (B) The axin mRNA expression in the thymus and TSCs is not altered in 12-month-old GHSR null mice.

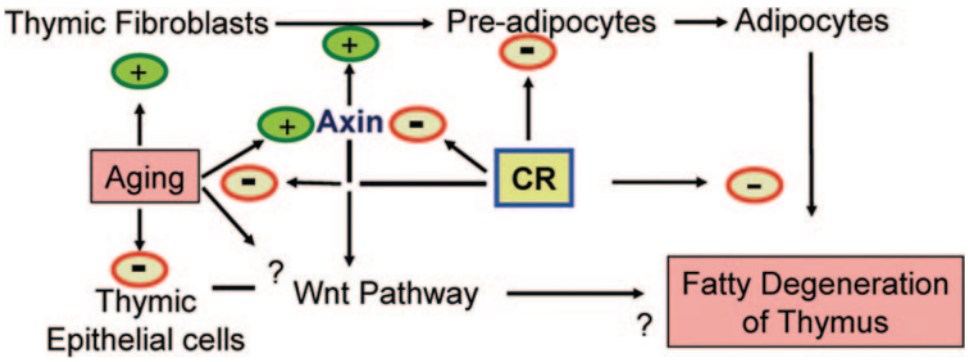

Fig. 9. Hypothetical model showing a role for axin in regulating thymic adiposity and involution. Aging leads to an increase in TF and a decrease in TEC, altering the TSC compositions. Increased expression of axin in TF induces adipogenesis, which may contribute to age-related accumulation of adipocytes in thymic space. CR maintains the thymic microenvironment by blocking the age-related increase in TF, reduced axin expression, and decreased thymic adiposity.

entiation into adipocytes, together with previous studies that axin overexpression reduces thymic cellularity [52], this suggests that increased axin with aging may promote thymic adipogenesis and involution (Fig. 9).

The neuroendocrine hormones that signal the state of negative energy balance induced by CR are believed to play an important role in mediating some of the complex prolongevity effects of CR [3, 49]. Ghrelin is induced post-CR and ghrelin infusions in old mice can partially reverse thymic involution [3, 4]. Similar to CR, ghrelin also inhibits inflammation [56, 57], although it remains unclear whether ghrelin mediates the pro-immune effects of CR. Interestingly, ablation of ghrelin signaling leads to an increase in proadipogenic regulators, such as PPARγ, aP2-4 (FABP4/aP2), CD36, and perilipin in the TSCs [58]. However, the aged GHSR null mice with accelerated thymic involution and thymic adiposity [4, 58] do not show an increase in axin expression in the thymus or TSCs, suggesting a distinct and specific regulatory mechanism.

These data suggest that ghrelin signaling via GHSR does not regulate the axin in the aging thymus. In addition, this also suggests that deficiency of ghrelin-mediated signaling and consequent thymic adiposity are under regulation of alternate regulatory pathways. Collectively, our data are consistent with the hypothesis that axin may play an important role in promoting the age-related thymic involution by increasing the adipocyte accumulation in the thymus. Thus, in addition to the present focus on regenerating the aging thymus by targeting lymphoid progenitors and TSCs, our findings suggest that cell-specific blocking of an age-related increase in proadipogenic regulators may significantly complement ongoing efforts to rejuvenate thymic function.

ACKNOWLEDGMENTS

The research work was supported in part by the Coypu Foundation and a grant from the NIH (AG031797) to V. D. D. The present work used the facilities of the Genomics and Cell Biology & Bioimaging (CBB) Core facilities supported by NIH Grant 1 P20 RR02/1945 and CBB Core Facility of the Pennington Center of Biomedical Research Excellence (NIH P20 RR-021945) and Clinical Nutrition Research Unit (NIH P30 DK072476). We thank Chiaki Nakata, Rachel Ohlmeyer, and Wubing Ye for technical assistance, Dr. Donald Ingram for thoughtful discussions, Dr. Roy Smith for providing the GHSR null mice, Dr. Gregory Sempowski for the mouse sjTREC plasmid, Dr. Richard Boyd for the generous gift of the MTS15 antibody, and Dr. Ann Chidgey for advice with TSC sorting procedures. We also thank Dr. Ping Zhang and Ms. Constance Porretta at Louisiana State University (LSU)-Health Science Center and Ms. Marilyn Dietrich at LSU School of Veterinary Medicine for FACS sorting.

REFERENCES

1. Linton, P. J., Dorshkind, K. (2004) Age-related changes in lymphocyte development and function. *Nat. Immunol.* **5,** 133–139.
2. Sutherland, J. S., Goldberg, G. L., Hammett, M. V., Uldrich, A. P., Berzins, S. P., Heng, T. S., Blazar, B. R., Millar, J. L., Malin, M. A., Chidgey, A. P., Boyd, R. L. (2005) Activation of thymic regeneration in mice and humans following androgen blockade. *J. Immunol.* **175,** 2741–2753.
3. Dixit, V. D. (2008) Adipose-immune interactions during obesity and caloric restriction: reciprocal mechanisms regulating immunity and health span. *J. Leukoc. Biol.* **84,** 882–892.
4. Dixit, V. D., Yang, H., Sun, Y., Weeraratna, A. T., Youm, Y. H., Smith, R. G., Taub, D. D. (2007) Ghrelin promotes thymopoiesis during aging. *J. Clin. Invest.* **117,** 2778–2790.
5. Gui, J., Zhu, X., Dohkan, J., Cheng, L., Barnes, P. F., Su, D. M. (2007) The aged thymus shows normal recruitment of lymphohematopoietic progenitors but has defects in thymic epithelial cells. *Int. Immunol.* **19,** 1201–1211.
6. Zhu, X., Gui, J., Dohkan, J., Cheng, L., Barnes, P. F., Su, D. M. (2007) Lymphohematopoietic progenitors do not have a synchronized defect with age-related thymic involution. *Aging Cell* **6,** 663–672.
7. Aw, D., Silva, A. B., Maddick, M., von Zglinicki, T., Palmer, D. B. (2008) Architectural changes in the thymus of aging mice. *Aging Cell* **7,** 158–167.
8. Chu, Y. W., Schmitz, S., Choudhury, B., Telford, W., Kapoor, V., Garfield, S., Howe, D., Gress, R. E. (2008) Exogenous insulin-like growth factor 1 enhances thymopoiesis predominantly through thymic epithelial cell expansion. *Blood* **112,** 2836–2846.
9. Min, D., Panoskaltsis-Mortari, A., Kuro-O, M., Holländer, G. A., Blazar, B. R., Weinberg, K. I. (2007) Sustained thymopoiesis and improvement in functional immunity induced by exogenous KGF administration in murine models of aging. *Blood* **109,** 2529–2537.
10. Min, H., Montecino-Rodriguez, E., Dorshkind, K. (2004) Reduction in the developmental potential of intrathymic T cell progenitors with age. *J. Immunol.* **173,** 245–250.
11. Chidgey, A., Dudakov, J., Seach, N., Boyd, R. (2007) Impact of niche aging on thymic regeneration and immune reconstitution. *Semin. Immunol.* **19,** 331–340.
12. Petrie, H. T., Zuniga-Pflucker, J. C. (2007) Zoned out: functional mapping of stromal signaling microenvironments in the thymus. *Annu. Rev. Immunol.* **25,** 649–679.
13. Steinmann, G. G. (1986) Changes in the human thymus during aging. *Curr. Top. Pathol.* **75,** 43–88.
14. Flores, K. G., Li, J., Sempowski, G. D., Haynes, B. F., Hale, L. P. (1999) Analysis of the human thymic perivascular space during aging. *J. Clin. Invest.* **104,** 1031–1039.
15. Pearse, G. (2006) Normal structure, function and histology of the thymus. *Toxicol. Pathol.* **34,** 504–514.

16. Manolagas, S. C., Almeida, M. (2007) Gone with the Wnts: β-catenin, T-cell factor, forkhead box O, and oxidative stress in age-dependent diseases of bone, lipid, and glucose metabolism. *Mol. Endocrinol.* **21,** 2605–2614.
17. Kléber, M., Sommer, L. (2004) Wnt signaling and the regulation of stem cell function. *Curr. Opin. Cell Biol.* **16,** 681–687.
18. Zeng, L., Fagotto, F., Zhang, T., Hsu, W., Vasicek, T. J., Perry III L., Lee, J. J., Tilghman, S. M., Gumbiner, B. M., Costantini, F. (1997) The mouse fused locus encodes Axin, an inhibitor of the Wnt signaling pathway that regulates embryonic axis formation. *Cell* **90,** 181–192.
19. Chia, I. V., Costantini, F. (2005) Mouse axin and axin2/conductin proteins are functionally equivalent in vivo. *Mol. Cell. Biol.* **25,** 4371–4376.
20. Reya, T., Clevers, H. (2005) Wnt signaling in stem cells and cancer. *Nature* **434,** 843–850.
21. Cadigan, K. M., Liu, Y. I. (2006) Wnt signaling: complexity at the surface. *J. Cell Sci.* **119,** 395–402.
22. Logan, C. Y., Nusse, R. (2004) The Wnt signaling pathway in development and disease. *Annu. Rev. Cell Dev. Biol.* **20,** 781–810.
23. Kawano, Y., Kypta, R. (2003) Secreted antagonists of the Wnt signaling pathway. *J. Cell Sci.* **116,** 2627–2634.
24. Weerkamp, F., Baert, M. R., Naber, B. A., Koster, E. E., de Haas, E. F., Atkuri, K. R., van Dongen, J. J., Herzenberg, L. A., Staal, F. J. (2006) Wnt signaling in the thymus is regulated by differential expression of intracellular signaling molecules. *Proc. Natl. Acad. Sci. USA* **103,** 3322–3326.
25. Liang, H., Coles, A. H., Zhu, Z., Zayas, J., Jurecic, R., Kang, J., Jones, S. N. (2007) Noncanonical Wnt signaling promotes apoptosis in thymocyte development. *J. Exp. Med.* **204,** 3077–3084.
26. van de Wetering, M., de Lau, W., Clevers, H. (2002) WNT signaling and lymphocyte development. *Cell* **109** (Suppl.), S13–S19.
27. Balciunaite, G., Keller, M. P., Balciunaite, E., Piali, L., Zuklys, S., Mathieu, Y. D., Gill, J., Boyd, R., Sussman, D. J., Holländer, G. A. (2002) Wnt glycoproteins regulate the expression of FoxN1, the gene defective in nude mice. *Nat. Immunol.* **3,** 1102–1108.
28. Staal, F. J., Clevers, H. C. (2003) Wnt signaling in the thymus. *Curr. Opin. Immunol.* **15,** 204–208.
29. de Geer, G., Webb, W. R., Gamsu, G. (1986) Normal thymus: assessment with MR and CT. *Radiology* **158,** 313–317.
30. Evans, R., Barish, G. D., Wang, Y. X. (2004) PPARs and the complex journey to obesity. *Nat. Med.* **10,** 355–361.
31. Rosen, E. D., MacDougald, O. A. (2006) Adipocyte differentiation from the inside out. *Nat. Rev. Mol. Cell Biol.* **7,** 885–896.
32. Tontonoz, P., Hu, E., Spiegelman, B. M. (1994) Stimulation of adipogenesis in fibroblasts by PPAR γ 2, a lipid-activated transcription factor. *Cell* **79,** 1147–1156.
33. Hotamisligil, G. S., Johnson, R. S., Distel, R. J., Ellis, R., Papaioannou, V. E., Spiegelman, B. M. (1996) Uncoupling of obesity from insulin resistance through a targeted mutation in aP2, the adipocyte fatty acid binding protein. *Science* **274,** 1377–1379.
34. Ross, S. E., Hemati, N., Longo, K. A., Bennett, C. N., Lucas, P. C., Erickson, R. L., MacDougald, O. A. (2000) Inhibition of adipogenesis by Wnt signaling. *Science* **289,** 950–953.
35. Liu, H., Fergusson, M. M., Castilho, R. M., Liu, J., Cao, L., Chen, J., Malide, D., Rovira, I. I., Schimel, D., Kuo, C. J., Gutkind, J. S., Hwang, P. M., Finkel, T. (2007) Augmented Wnt signaling in a mammalian model of accelerated aging. *Science* **317,** 803–806.
36. Brack, A. S., Conboy, M. J., Roy, S., Lee, M., Kuo, C. J., Keller, C., Rando, T. A. (2007) Increased Wnt signaling during aging alters muscle stem cell fate and increases fibrosis. *Science* **317,** 807–810.
37. Ye, X., Zerlanko, B., Kennedy, A., Banumathy, G., Zhang, R., Adams, P. D. (2007) Downregulation of Wnt signaling is a trigger for formation of facultative heterochromatin and onset of cell senescence in primary human cells. *Mol. Cell* **27,** 183–196.
38. Strutz, F., Okada, H., Lo, C. W., Danoff, T., Carone, R. L., Tomaszewski, J. E., Neilson, E. G. (1995) Identification and characterization of a fibroblast marker: FSP1. *J. Cell Biol.* **130,** 393–405.
39. Iwano, M., Plieth, D., Danoff, T. M., Xue, C., Okada, H., Neilson, E. G. (2002) Evidence that fibroblasts derive from epithelium during tissue fibrosis. *J. Clin. Invest.* **110,** 341–350.
40. Douek, D. C., McFarland, R. D., Keiser, P. H., Gage, E. A., Massey, J. M., Haynes, B. F., Polis, M. A., Haase, A. T., Feinberg, M. B., Sullivan, J. L., Jamieson, B. D., Zack, J. A., Picker, L. J., Koup, R. A. (1998) Changes in thymic function with age and during the treatment of HIV infection. *Nature* **396,** 690–695.
41. Van den Dool, C., de Boer, R. J. (2006) The effects of age, thymectomy, and HIV infection on α and β TCR excision circles in naive T cells. *J. Immunol.* **177,** 4391–4401.
42. Wharton Jr., K. A., Zimmermann, G., Rousset, R., Scott, M. P. (2001) Vertebrate proteins related to Drosophila naked cuticle bind disheveled and antagonize Wnt signaling. *Dev. Biol.* **234,** 93–106.
43. Van Raay, T. J., Coffey, R. J., Solnica-Krezel, L. (2007) Zebrafish Naked1 and Naked2 antagonize both canonical and non-canonical Wnt signaling. *Dev. Biol.* **309,** 151–168.
44. Smas, C. M., Sul, H. S. (1993) Pref-1, a protein containing EGF-like repeats, inhibits adipocyte differentiation. *Cell* **73,** 725–734.
45. Moon, Y. S., Smas, C. M., Lee, K., Villena, J. A., Kim, K. H., Yun, E. J., Sul, H. S. (2002) Mice lacking paternally expressed Pref-1/Dlk1 display growth retardation and accelerated adiposity. *Mol. Cell. Biol.* **22,** 5585–5592.
46. Lee, K., Villena, J. A., Moon, Y. S., Kim, K. H., Lee, S., Kang, C., Sul, H. S. (2003) Inhibition of adipogenesis and development of glucose intolerance by soluble preadipocyte factor-1 (Pref-1). *J. Clin. Invest.* **111,** 453–461.
47. Yang, H., Youm, Y. H., Nakata, C., Dixit, V. D. (2007) Chronic caloric restriction induces forestomach hypertrophy with enhanced ghrelin levels during aging. *Peptides* **28,** 1931–1936.
48. Zediak, V. P., Maillard, I., Bhandoola, A. (2007) Multiple prethymic defects underlie age related loss of T progenitor competence. *Blood* **110,** 1161–1167.
49. Anderson, G., Jenkinson, E. J. (2001) Lymphostromal interactions in thymic development and function. *Nat. Rev. Immunol.* **1,** 31–40.
50. Hale, J. S., Boursalian, T. E., Turk, G. L., Fink, P. J. (2006) Thymic output in aged mice. *Proc. Natl. Acad. Sci. USA* **103,** 8447–8452.
51. Bhandoola, A., von Boehmer, H., Petrie, H. T., Zuniga-Pflucker, J. C. (2007) Commitment and developmental potential of extrathymic and intrathymic T cell precursors: plenty to choose from. *Immunity* **26,** 678–689.
52. Hsu, W., Shakya, R., Costantini, F. (2001) Impaired mammary gland and lymphoid development caused by inducible expression of Axin in transgenic mice. *J. Cell Biol.* **155,** 1055–1064.
53. Mohtashami, M., Zúñiga-Pflücker, J. C. (2005) Three-dimensional architecture of the thymus is required to maintain δ-like expression necessary for inducing T cell development. *J. Immunol.* **175,** 4858–4865.
54. Nikolich-Zugich, J., Messaoudi, I. (2005) Mice and flies and monkeys too: caloric restriction rejuvenates the aging immune system of non-human primates. *Exp. Gerontol.* **40,** 884–893.
55. Messaoudi, I., Warner, J., Fischer, M., Park, B., Hill, B., Mattison, J., Lane, M. A., Roth, G. S., Ingram, D. K., Picker, L. J., Douek, D. C., Mori, M., Nikolich-Zugich, J. (2006) Delay of T cell senescence by caloric restriction in aged long-lived nonhuman primates. *Proc. Natl. Acad. Sci. USA* **103,** 19448–19453.
56. Dixit, V. D., Schaffer, E. M., Pyle, R. S., Collins, G. D., Sakthivel, S. K., Palaniappan, R., Lillard Jr., J. W., Taub, D. D. (2004) Ghrelin inhibits leptin- and activation-induced proinflammatory cytokine expression by human monocytes and T cells. *J. Clin. Invest.* **114,** 57–66.
57. Li, W. G., Gavrila, D., Liu, X., Wang, L., Gunnlaugsson, S., Stoll, L. L., McCormick, M. L., Sigmund, C. D., Tang, C., Weintraub, N. L. (2004) Ghrelin inhibits proinflammatory responses and nuclear factor-κB activation in human endothelial cells. *Circulation* **109,** 2221–2226.
58. Youm, Y. H., Yang, H., Sun, Y., Smith, R. G., Manley, N. R., Vandanmagsar, B., Dixit, V. D. (2009) Deficient ghrelin receptor mediated signaling compromises thymic stromal cell microenvironment by accelerating thymic adiposity. *J. Biol. Chem.* **284,** 7068–7077.